

EUROPEAN ORGANISATION FOR NUCLEAR RESEARCH (CERN)

CERN-EP/2000-052

11 April 2000

Measurement of W-pair production in e^+e^- collisions at 189 GeV

The ALEPH Collaboration

Abstract

The production of W^+W^- pairs is analysed in a data sample collected by ALEPH at a mean centre-of-mass energy of 188.6 GeV, corresponding to an integrated luminosity of 174.2 pb^{-1} . Cross sections are given for different topologies of W decays into leptons or hadrons. Combining all final states and assuming Standard Model branching fractions, the total W-pair cross section is measured to be $15.71 \pm 0.34(\text{stat.}) \pm 0.18(\text{syst.}) \text{ pb}$. Using also the W-pair data samples collected by ALEPH at lower centre-of-mass energies, the decay branching fraction of the W boson into hadrons is measured to be $B(W \rightarrow \text{hadrons}) = 66.97 \pm 0.65(\text{stat.}) \pm 0.32(\text{syst.})\%$, allowing a determination of the CKM matrix element $|V_{cs}| = 0.951 \pm 0.030(\text{stat.}) \pm 0.015(\text{syst.})$.

(Submitted to Physics Letters B)

The ALEPH Collaboration

R. Barate, D. Decamp, P. Ghez, C. Goy, S. Jezequel, J.-P. Lees, F. Martin, E. Merle, M.-N. Minard, B. Pietrzyk

Laboratoire de Physique des Particules (LAPP), IN²P³-CNRS, F-74019 Annecy-le-Vieux Cedex, France

R. Alemany, S. Bravo, M.P. Casado, M. Chmeissani, J.M. Crespo, E. Fernandez, M. Fernandez-Bosman, Ll. Garrido,¹⁵ E. Graugés, M. Martinez, G. Merino, R. Miquel, Ll.M. Mir, A. Pacheco, H. Ruiz

Institut de Física d'Altes Energies, Universitat Autònoma de Barcelona, E-08193 Bellaterra (Barcelona), Spain⁷

A. Colaleo, D. Creanza, M. de Palma, G. Iaselli, G. Maggi, M. Maggi, S. Nuzzo, A. Ranieri, G. Raso, F. Ruggieri, G. Selvaggi, L. Silvestris, P. Tempesta, A. Tricomi,³ G. Zito

Dipartimento di Fisica, INFN Sezione di Bari, I-70126 Bari, Italy

X. Huang, J. Lin, Q. Ouyang, T. Wang, Y. Xie, R. Xu, S. Xue, J. Zhang, L. Zhang, W. Zhao

Institute of High Energy Physics, Academia Sinica, Beijing, The People's Republic of China⁸

D. Abbaneo, G. Boix,⁶ O. Buchmüller, M. Cattaneo, F. Cerutti, G. Dissertori, H. Drevermann, R.W. Forty, M. Frank, F. Gianotti, T.C. Greening, A.W. Halley, J.B. Hansen, J. Harvey, P. Janot, B. Jost, M. Kado, V. Lemaître, P. Maley, P. Mato, A. Minten, A. Moutoussi, F. Ranjard, L. Rolandi, D. Schlatter, M. Schmitt,²⁰ O. Schneider,² P. Spagnolo, W. Tejessy, F. Teubert, E. Tournefier, A. Valassi, J.J. Ward, A.E. Wright

European Laboratory for Particle Physics (CERN), CH-1211 Geneva 23, Switzerland

Z. Ajaltouni, F. Badaud, G. Chazelle, O. Deschamps, S. Dessagne, A. Falvard, P. Gay, C. Guicheney, P. Henrard, J. Jousset, B. Michel, S. Monteil, J.-C. Montret, D. Pallin, J.M. Pascolo, P. Perret, F. Podlyski

Laboratoire de Physique Corpusculaire, Université Blaise Pascal, IN²P³-CNRS, Clermont-Ferrand, F-63177 Aubière, France

J.D. Hansen, J.R. Hansen, P.H. Hansen,¹ B.S. Nilsson, A. Wäänänen

Niels Bohr Institute, 2100 Copenhagen, DK-Denmark⁹

G. Daskalakis, A. Kyriakis, C. Markou, E. Simopoulou, A. Vayaki

Nuclear Research Center Demokritos (NRCD), GR-15310 Attiki, Greece

A. Blondel,¹² J.-C. Brient, F. Machefert, A. Rougé, M. Swynghedauw, R. Tanaka H. Videau

Laboratoire de Physique Nucléaire et des Hautes Energies, Ecole Polytechnique, IN²P³-CNRS, F-91128 Palaiseau Cedex, France

E. Focardi, G. Parrini, K. Zachariadou

Dipartimento di Fisica, Università di Firenze, INFN Sezione di Firenze, I-50125 Firenze, Italy

A. Antonelli, G. Bencivenni, G. Bologna,⁴ F. Bossi, P. Campana, G. Capon, V. Chiarella, P. Laurelli, G. Mannocchi,^{1,5} F. Murtas, G.P. Murtas, L. Passalacqua, M. Pepe-Altarelli

Laboratori Nazionali dell'INFN (LNF-INFN), I-00044 Frascati, Italy

M. Chalmers, J. Kennedy, J.G. Lynch, P. Negus, V. O'Shea, B. Raeven, D. Smith, P. Teixeira-Dias, A.S. Thompson

Department of Physics and Astronomy, University of Glasgow, Glasgow G12 8QQ, United Kingdom¹⁰

R. Cavanaugh, S. Dhamotharan, C. Geweniger,¹ P. Hanke, V. Hepp, E.E. Kluge, G. Leibenguth, A. Putzer, K. Tittel, S. Werner,¹⁹ M. Wunsch¹⁹

Kirchhoff-Institut für Physik, Universität Heidelberg, D-69120 Heidelberg, Germany¹⁶

R. Beuselinck, D.M. Binnie, W. Cameron, G. Davies, P.J. Dornan, M. Girone, N. Marinelli, J. Nowell, H. Przysiezniak,¹ J.K. Sedgbeer, J.C. Thompson,¹⁴ E. Thomson,²³ R. White

Department of Physics, Imperial College, London SW7 2BZ, United Kingdom¹⁰

V.M. Ghete, P. Girtler, E. Kneringer, D. Kuhn, G. Rudolph

Institut für Experimentalphysik, Universität Innsbruck, A-6020 Innsbruck, Austria¹⁸

C.K. Bowdery, P.G. Buck, D.P. Clarke, G. Ellis, A.J. Finch, F. Foster, G. Hughes, R.W.L. Jones, N.A. Robertson, M. Smizanska

Department of Physics, University of Lancaster, Lancaster LA1 4YB, United Kingdom¹⁰

I. Giehl, F. Hölldorfer, K. Jakobs, K. Kleinknecht, M. Kröcker, A.-S. Müller, H.-A. Nürnbergger, G. Quast,¹ B. Renk, E. Rohne, H.-G. Sander, S. Schmeling, H. Wachsmuth, C. Zeitnitz, T. Ziegler

Institut für Physik, Universität Mainz, D-55099 Mainz, Germany¹⁶

A. Bonissent, J. Carr, P. Coyle, C. Curtil, A. Ealet, D. Fouchez, O. Leroy, T. Kachelhoffer, P. Payre, D. Rousseau, A. Tilquin

Centre de Physique des Particules de Marseille, Univ Méditerranée, IN²P³-CNRS, F-13288 Marseille, France

M. Aleppo, M. Antonelli, S. Gilardoni, F. Ragusa

Dipartimento di Fisica, Università di Milano e INFN Sezione di Milano, I-20133 Milano, Italy.

H. Dietl, G. Ganis, K. Hüttmann, G. Lütjens, C. Mannert, W. Männer, H.-G. Moser, S. Schael, R. Settles,¹ H. Stenzel, W. Wiedenmann, G. Wolf

Max-Planck-Institut für Physik, Werner-Heisenberg-Institut, D-80805 München, Germany¹⁶

P. Azzurri, J. Boucrot,¹ O. Callot, M. Davier, L. Dufflot, J.-F. Grivaz, Ph. Heusse, A. Jacholkowska,¹ L. Serin, J.-J. Veillet, I. Videau,¹ J.-B. de Vivie de Régie, D. Zerwas

Laboratoire de l'Accélérateur Linéaire, Université de Paris-Sud, IN²P³-CNRS, F-91898 Orsay Cedex, France

G. Bagliesi, T. Boccali, G. Calderini, V. Ciulli, L. Foà, A. Giassi, F. Ligabue, A. Messineo, F. Palla,¹ G. Rizzo, G. Sanguinetti, A. Sciabà, G. Sguazzoni, R. Tenchini,¹ A. Venturi, P.G. Verdini

Dipartimento di Fisica dell'Università, INFN Sezione di Pisa, e Scuola Normale Superiore, I-56010 Pisa, Italy

G.A. Blair, J. Coles, G. Cowan, M.G. Green, D.E. Hutchcroft, L.T. Jones, T. Medcalf, J.A. Strong, J.H. von Wimmersperg-Toeller

Department of Physics, Royal Holloway & Bedford New College, University of London, Surrey TW20 OEX, United Kingdom¹⁰

R.W. Clifft, T.R. Edgecock, P.R. Norton, I.R. Tomalin

Particle Physics Dept., Rutherford Appleton Laboratory, Chilton, Didcot, Oxon OX11 0QX, United Kingdom¹⁰

B. Bloch-Devaux, P. Colas, B. Fabbro, G. Faïf, E. Lançon, M.-C. Lemaire, E. Locci, P. Perez, J. Rander, J.-F. Renardy, A. Rosowsky, P. Seager,¹³ A. Trabelsi,²¹ B. Tuchming, B. Vallage

CEA, DAPNIA/Service de Physique des Particules, CE-Saclay, F-91191 Gif-sur-Yvette Cedex, France¹⁷

S.N. Black, J.H. Dann, C. Loomis, H.Y. Kim, N. Konstantinidis, A.M. Litke, M.A. McNeil, G. Taylor

Institute for Particle Physics, University of California at Santa Cruz, Santa Cruz, CA 95064, USA²²

C.N. Booth, S. Cartwright, F. Combley, P.N. Hodgson, M. Lehto, L.F. Thompson

Department of Physics, University of Sheffield, Sheffield S3 7RH, United Kingdom¹⁰

K. Affholderbach, A. Böhrer, S. Brandt, C. Grupen, J. Hess, A. Misiejuk, G. Prange, U. Sieler

Fachbereich Physik, Universität Siegen, D-57068 Siegen, Germany¹⁶

C. Borean, G. Giannini, B. Gobbo

Dipartimento di Fisica, Università di Trieste e INFN Sezione di Trieste, I-34127 Trieste, Italy

H. He, J. Putz, J. Rothberg, S. Wasserbaech

Experimental Elementary Particle Physics, University of Washington, WA 98195 Seattle, U.S.A.

S.R. Armstrong, K. Cranmer, P. Elmer, D.P.S. Ferguson, Y. Gao, S. González, O.J. Hayes, H. Hu, S. Jin, J. Kile, P.A. McNamara III, J. Nielsen, W. Orejudos, Y.B. Pan, Y. Saadi, I.J. Scott, J. Walsh, J. Wu, Sau Lan Wu, X. Wu, G. Zobernig

Department of Physics, University of Wisconsin, Madison, WI 53706, USA¹¹

¹Also at CERN, 1211 Geneva 23, Switzerland.

²Now at Université de Lausanne, 1015 Lausanne, Switzerland.

³Also at Dipartimento di Fisica di Catania and INFN Sezione di Catania, 95129 Catania, Italy.

⁴Also Istituto di Fisica Generale, Università di Torino, 10125 Torino, Italy.

⁵Also Istituto di Cosmo-Geofisica del C.N.R., Torino, Italy.

⁶Supported by the Commission of the European Communities, contract ERBFMBICT982894.

⁷Supported by CICYT, Spain.

⁸Supported by the National Science Foundation of China.

⁹Supported by the Danish Natural Science Research Council.

¹⁰Supported by the UK Particle Physics and Astronomy Research Council.

¹¹Supported by the US Department of Energy, grant DE-FG0295-ER40896.

¹²Now at Département de Physique Corpusculaire, Université de Genève, 1211 Genève 4, Switzerland.

¹³Supported by the Commission of the European Communities, contract ERBFMBICT982874.

¹⁴Also at Rutherford Appleton Laboratory, Chilton, Didcot, UK.

¹⁵Permanent address: Universitat de Barcelona, 08208 Barcelona, Spain.

¹⁶Supported by the Bundesministerium für Bildung, Wissenschaft, Forschung und Technologie, Germany.

¹⁷Supported by the Direction des Sciences de la Matière, C.E.A.

¹⁸Supported by the Austrian Ministry for Science and Transport.

¹⁹Now at SAP AG, 69185 Walldorf, Germany

²⁰Now at Harvard University, Cambridge, MA 02138, U.S.A.

²¹Now at Département de Physique, Faculté des Sciences de Tunis, 1060 Le Belyvédère, Tunisia

1 Introduction

This letter presents results on W-pair production in e^+e^- collisions using data collected with the ALEPH detector at a centre-of-mass (CM) energy around 189 GeV, during the 1998 data taking period. The WW events are identified in all possible W decay channels, thus allowing the determination of the W branching fractions and indirectly, the coupling of the W to cs pairs.

The experimental conditions and data analysis follow those used in the cross section measurements at lower LEP2 energies. As they are already described in detail in [1], attention is focused here on changes to selection procedures other than a simple rescaling of cuts with the increased collision energy.

A detailed description of the ALEPH detector can be found in Ref. [2] and of its performance in Ref. [3]. The luminosity is measured from small-angle Bhabha events, using lead-proportional wire sampling calorimeters [4], with an accepted Bhabha cross section of approximately 4.25 nb [5]. An integrated luminosity of 174.20 ± 0.20 (stat.) ± 0.73 (syst.) pb^{-1} was recorded at a mean CM energy of 188.63 ± 0.04 GeV [6].

In this letter, the quoted signal cross sections are the CC03 cross sections [7], defined as the production of four-fermion final states through two resonating W bosons. Two processes contribute, ν_e exchange in the t -channel and Z/γ exchange in the s -channel. The measured cross sections are corrected for the difference, denoted the “4f-CC03 correction” [1], between the accepted cross sections for CC03 processes and all Standard Model four-fermion final states consistent with W-pair decays.

The CC03 Standard Model cross section (σ_{WW}), calculated at $\sqrt{s} = 188.63$ GeV with the program GENTLE [8] is 16.65 pb ($\pm 2\%$). The KORALW [9] version 1.21 Monte Carlo event generator is used to simulate the signal events with a normalised cross section in agreement with the GENTLE value. The JETSET [10] package is used for the hadronisation. Comparison samples, generated with EXCALIBUR [11] and grc4f [12] for both CC03 and all four-fermion diagrams, are used for systematic error evaluation. Samples of events are also generated with different W masses, both for CC03 diagrams and for all WW-like four-fermion diagrams, with KORALW.

The KORALZ [13] Monte Carlo program is used to generate $e^+e^- \rightarrow q\bar{q}$ background events. Other backgrounds are generated with PYTHIA 5.7 [14] for ZZ, Zee and $W\ell\nu$ processes, PHOTO2 [15] for $\gamma\gamma$ interactions, KORALZ for μ and τ pair production and BHWIDE [16] and UNIBAB [17] for Bhabha events.

2 Selection of W-pair candidates

2.1 WW $\rightarrow l\nu l\nu$ events

The selection of fully leptonic W-pair decays follows exactly the two selections used for the cross section and branching fraction measurements at 183 GeV [1]. The two selections have similar overall efficiencies and background levels but differ in their sensitivities to the individual dilepton channels. The first is based on topological information and is sensitive to all channels. In the second, lepton identification is used to optimise the cuts according

to which final state is being considered. Events are accepted as WW candidates if they pass either of the two selections and are then classified into six di-lepton channels making use of electron and muon identification criteria. A jet or a single charged particle track is classified as a tau if no lepton is identified or the identified lepton has an energy less than 25 GeV.

Beam related background, not simulated in Monte Carlo events, affects the efficiency of the cut which removes events depositing energy within 12° of the beam. Random trigger events were used to model these local energy deposits close to the beam. The inefficiency introduced is found to be $8.2 \pm 0.5\%$. The CC03 efficiencies in the individual $l\nu l\nu$ channels are given in Table 1 after correction for this beam related effect. The inclusive combination of the two selections has an overall efficiency of $64.2 \pm 0.4\%$ for the fully leptonic channels when combined assuming lepton universality. The total background amounts to $131 \pm 7(\text{stat.}) \pm 8.5(\text{syst.})$ fb and is dominated by $\gamma\gamma \rightarrow \ell\ell$ and non-WW-like $ZZ \rightarrow \ell l\nu\nu$ events. In the data, the inclusive combination selects 220 events.

All sources of systematic uncertainties are listed in Table 2. They are dominated by the uncertainties on the background cross sections, the uncertainty from the cut on energy detected close to the beam and by Monte Carlo statistics.

A maximum likelihood fit is applied to determine the cross section for each fully leptonic decay channel using the efficiency matrices for signal and backgrounds given in Table 1. For all channels together the 4f-CC03 correction is -10 ± 10 fb, where the uncertainty comes from Monte Carlo statistics.

The results of the fit are

$$\begin{aligned}
\sigma(\text{WW} \rightarrow e\nu e\nu) &= 0.19 \pm 0.05(\text{stat.}) \pm 0.01(\text{syst.}) \text{ pb}, \\
\sigma(\text{WW} \rightarrow \mu\nu\mu\nu) &= 0.20 \pm 0.05(\text{stat.}) \pm 0.01(\text{syst.}) \text{ pb}, \\
\sigma(\text{WW} \rightarrow \tau\nu\tau\nu) &= 0.22 \pm 0.08(\text{stat.}) \pm 0.02(\text{syst.}) \text{ pb}, \\
\sigma(\text{WW} \rightarrow e\nu\mu\nu) &= 0.43 \pm 0.07(\text{stat.}) \pm 0.01(\text{syst.}) \text{ pb}, \\
\sigma(\text{WW} \rightarrow e\nu\tau\nu) &= 0.36 \pm 0.08(\text{stat.}) \pm 0.02(\text{syst.}) \text{ pb}, \\
\sigma(\text{WW} \rightarrow \mu\nu\tau\nu) &= 0.38 \pm 0.08(\text{stat.}) \pm 0.01(\text{syst.}) \text{ pb}.
\end{aligned}$$

The systematic uncertainties are obtained by varying all input parameters in the fit according to their uncertainties.

The total fully leptonic cross section is obtained with the same fit, assuming lepton universality:

$$\sigma(\text{WW} \rightarrow l\nu l\nu) = 1.78 \pm 0.13(\text{stat.}) \pm 0.02(\text{syst.}) \text{ pb},$$

consistent with the sum of the individual channels.

2.2 WW $\rightarrow l\nu q\bar{q}$ events

As for the lower energy measurements, three $l\nu q\bar{q}$ selection procedures are applied. One selection requires an identified electron or muon. The other two are designed to select $\tau\nu q\bar{q}$ events, based on global variables or topological properties of the events.

The selection of $e\nu q\bar{q}$ and $\mu\nu q\bar{q}$ events has been modified with respect to the previous analysis [1] to take into account the greater initial boost of the W's. The preselection

Table 1: Summary of results of the different event selections on Monte Carlo and data events. Efficiencies are given in percent of CC03 processes; they assume Standard Model branching fractions in the overall values quoted in the right-hand column. The $q\bar{q}q\bar{q}$ column refers to events with a NN output greater than 0.3 where the backgrounds also include non- $q\bar{q}q\bar{q}$ WW decays. The listed backgrounds do not include the 4f-CC03 corrections.

		Event selection and classification										All
		ee	$e\mu$	$e\tau$	$\mu\mu$	$\mu\tau$	$\tau\tau$	$eq\bar{q}$	$\mu q\bar{q}$	$\tau q\bar{q}$	$q\bar{q}q\bar{q}$	
Eff. for WW→ (%)	$e\nu e\nu$	57.8	-	8.8	-	-	0.5	-	-	-	-	67.1
	$e\nu\mu\nu$	-	59.0	4.7	-	4.6	0.3	-	-	-	-	68.6
	$e\nu\tau\nu$	3.0	4.2	50.1	-	0.3	4.3	-	-	-	-	61.9
	$\mu\nu\mu\nu$	-	-	-	61.9	8.3	0.3	-	-	-	-	70.6
	$\mu\nu\tau\nu$	-	4.2	0.3	3.5	52.9	3.5	-	-	-	-	64.4
	$\tau\nu\tau\nu$	0.2	0.4	7.7	0.4	6.0	36.5	-	-	-	-	51.2
	$e\nu q\bar{q}$	-	-	-	-	-	-	82.4	-	5.4	0.2	88.0
	$\mu\nu q\bar{q}$	-	-	-	-	-	-	-	87.5	4.1	0.2	91.9
	$\tau\nu q\bar{q}$	-	-	-	-	-	-	3.7	3.8	59.0	0.9	68.0
	$q\bar{q}q\bar{q}$	-	-	-	-	-	-	-	-	-	91.7	91.7
Expected background events	3	1	7	2	3	6	17	5	33	323	400	
Observed Events	24	51	48	26	46	25	381	382	303	1435	2721	

remains similar. It is based on the total charged particle energy and multiplicity and a cut on the longitudinal momentum and visible energy to reject $Z\gamma$ events with an undetected photon. The selection of the lepton track relies on the fact that it is in general more energetic and isolated than the charged particles from the hadronic system. Thus the candidate lepton is chosen as the charged track that maximises $p_\ell^2(1 - \cos\theta_{\ell j})$, where p_ℓ is the track momentum and $\theta_{\ell j}$ the angle of the track to the closest of the jets clustered using the remaining reconstructed charged particles. For the jet clustering the DURHAM-P [18] algorithm with a y_{cut} of 0.0003 is used.

The same electron or muon identification criteria as for the fully leptonic channels are required for this lepton candidate track. However, no cut is applied on the lepton energy, so that $\tau\nu q\bar{q}$ events where the τ decays to a softer lepton (as $\tau \rightarrow e\nu\nu$ or $\tau \rightarrow \mu\nu\nu$) are also selected by this analysis.

For electron candidates the lepton energy is corrected for possible bremsstrahlung photons detected in the electromagnetic calorimeter. The isolation of the lepton is defined as $\log(\tan\theta_C/2) + \log(\tan\theta_F/2)$ where θ_C and θ_F are, respectively, the angle of the lepton to the closest charged track, and the opening angle of the largest cone centred on the lepton direction which contains a total energy smaller than 5 GeV.

For each event, probabilities that it comes from each of the three signal processes, $e\nu q\bar{q}$, $\mu\nu q\bar{q}$ or $\tau\nu q\bar{q}$, are determined (Fig. 1) using Monte Carlo reference samples of

signal and backgrounds. These are evaluated from the identity, energy and isolation of the lepton plus the event total transverse momentum. An event is classified as $e\nu q\bar{q}$ or $\mu\nu q\bar{q}$ if its corresponding probability is greater than 0.40; it is then not considered in the tau search.

The selection of $\tau\nu q\bar{q}$ events is based both on global event variables and a topological selection which attempts to identify the τ jet. As the selections were described in detail in previous papers [1], only changes other than a rescaling of the values of the energy-based cuts are described in the following:

- (i) in the global analysis the visible mass is required to be greater than $85 \text{ GeV}/c^2$ and less than $155 \text{ GeV}/c^2$ to take account of the boost of the W boson. The estimated energy of the “primary” neutrino must be smaller than 70 GeV;
- (ii) in the topological analysis, the energy of the most energetic quark jet must be less than 75 GeV and the mass of the hadronic system, i.e., the mass excluding the tau jet, is required to be less than $100 \text{ GeV}/c^2$.

In addition, if an event with a well defined e or μ fails the e/μ probability cut it is considered as a τ candidate and kept if the $\tau\nu q\bar{q}$ probability (Fig. 1c) is greater than 0.4.

Table 2: Systematic error summary (units in fb)

Source	WW cross section		
	$l\nu l\nu$	$l\nu q\bar{q}$	$q\bar{q}q\bar{q}$
Calibration of calorimeters			32
Jet calibrations			9
WW generator and m_W dependence			25
WW fragmentation			17
Lepton isolation		56	
$q\bar{q}$ generator			23
Background shape			50
Final state interactions			38
Background normalisation	13	30	84
Luminosity	9	35	39
Monte Carlo statistics	15	61	36
Beam related background	11	30	40
Lepton identification	2	45	
Probability cut		46	
Total	24	118	134

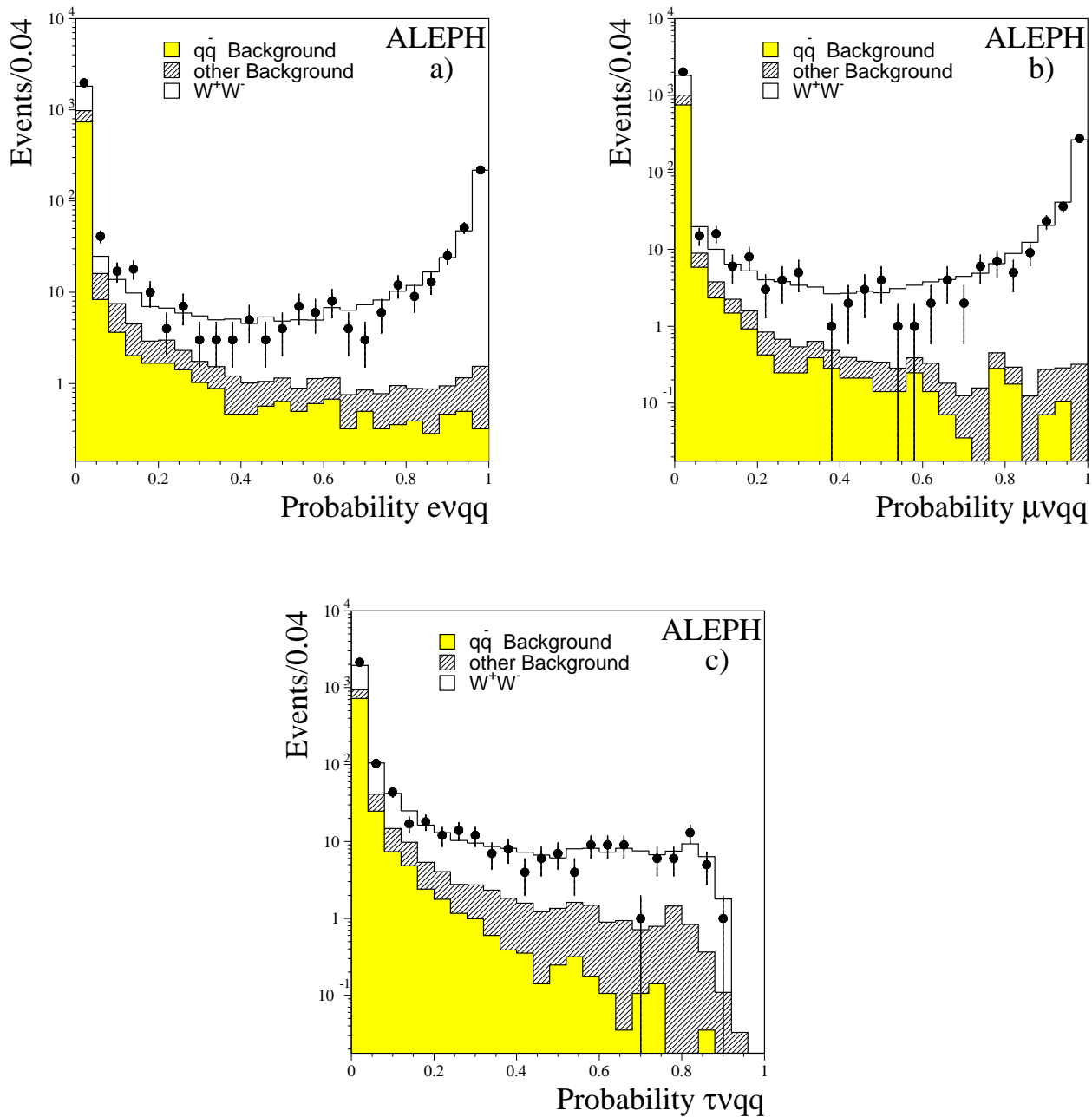


Figure 1: Probability distributions of preselected events for the (a) $\nu_e \nu_q \bar{q}$, (b) $\mu \nu_q \bar{q}$ and (c) $\tau \nu_q \bar{q}$ selections. The points are the data and the histograms the Monte Carlo predictions. The non- $q\bar{q}$ backgrounds include ZZ , Zee , $We\nu$ and $\tau^+\tau^-$ processes.

2.2.1 Results

Table 1 gives the efficiencies for each selection. The inclusive efficiencies for the three semileptonic decay channels are $87.8 \pm 0.4\%$ for the electron channel, $91.6 \pm 0.4\%$ for the muon channel and $66.5 \pm 0.5\%$ for the tau channel, giving an $82 \pm 0.3\%$ average efficiency for $WW \rightarrow \ell\nu q\bar{q}$, with a background of $314 \pm 12(\text{stat.}) \pm 25(\text{syst.})$ fb. The overall 4f-CC03 correction is $+8 \pm 40$ fb. A total of 1066 events are selected in the data.

The systematic uncertainties on the combined semileptonic cross section are summarised in Table 2. The largest contribution arises from the Monte Carlo statistical error on the 4f-CC03 correction. Uncertainties arising from the choice of the lepton isolation criterium and the probability cut are estimated from the change of efficiency following a bin-by-bin reweighting of the respective Monte Carlo one-dimensional distributions to the data. Background normalisation mainly affects the tau channel although there is also a contribution from residual Bhabha background in the electron channel. Decays of the Z to electrons and muons are used to evaluate lepton identification uncertainties whilst the contribution from beam related backgrounds is estimated by superimposing the energy deposits from random triggers on to the simulated events.

To evaluate the individual cross sections a similar fit as for the fully leptonic events is used with the corresponding matrix of efficiencies and backgrounds. This yields

$$\begin{aligned}\sigma(WW \rightarrow e\nu q\bar{q}) &= 2.41 \pm 0.14(\text{stat.}) \pm 0.07(\text{syst.}) \text{ pb}, \\ \sigma(WW \rightarrow \mu\nu q\bar{q}) &= 2.39 \pm 0.13(\text{stat.}) \pm 0.06(\text{syst.}) \text{ pb}, \\ \sigma(WW \rightarrow \tau\nu q\bar{q}) &= 2.23 \pm 0.17(\text{stat.}) \pm 0.08(\text{syst.}) \text{ pb},\end{aligned}$$

where the systematic uncertainties are obtained by varying all input parameters of the fit according to their uncertainties.

The total $\ell\nu q\bar{q}$ cross section is extracted by means of the same fit, under the assumption of lepton universality:

$$\sigma(WW \rightarrow \ell\nu q\bar{q}) = 7.07 \pm 0.23(\text{stat.}) \pm 0.12(\text{syst.}) \text{ pb},$$

again consistent with a simple sum of the three channels.

2.3 $WW \rightarrow q\bar{q}q\bar{q}$ events

The analysis of WW decays to four jets is updated from Ref. [1] and consists of a simple preselection followed by a fit to the distribution of the output of a neural network (NN) with 14 input variables.

In the preselection, the first step is to remove events with a large undetected initial state (ISR) photon from radiative returns to the Z by requiring that the modulus of the total longitudinal momentum of all objects is less than $1.5(M_{vis} - M_Z)$ where M_{vis} is the observed visible mass. The particles are then forced into four jets using the DURHAM-PE algorithm [18] and the value of y_{34} , where a four-jet event becomes a three-jet event, is required to be greater than 0.001. To reject $q\bar{q}$ events with a visible ISR photon none of the four jets can have more than 95% of electromagnetic energy in a one degree cone around any particle included in the jet. Four-fermion final states where one of the fermions

is a charged lepton are rejected by requiring that the maximum energy fraction of a single charged particle in a jet be smaller than 0.9.

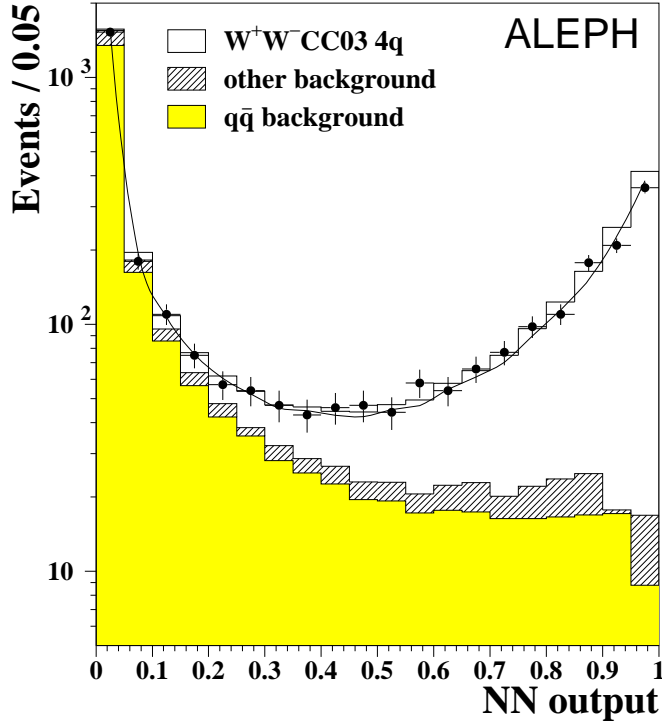


Figure 2: Comparison of NN output distributions for data and Monte Carlo after the four-quark preselection. The points are the data and the histograms the Monte Carlo predictions. The line shows the fit result.

At this point, 3438 events are selected in the data while 3593 ± 7 events are expected from Standard Model processes. This preselection has an efficiency of 98.4% for CC03 events and a purity of 35.9%.

The input variables for the NN are described in the Appendix and are related to the global event properties, the properties of jets, WW kinematics and the b-tag probabilities for the four jets. The NN is simplified with respect to that used for the analysis of the 183 GeV data [1], with fewer input variables and a slightly improved performance. The output distributions of the NN for the data compared with the signal and backgrounds predicted by the Monte Carlo are given in Fig. 2. In Table 1 results are given for a cut at 0.3 on the NN value.

The cross section is extracted by means of a binned maximum likelihood fit to the full NN output distribution. In the fit only the normalisation of the Monte Carlo signal is allowed to vary; all backgrounds, including $WW \rightarrow \ell\nu q\bar{q}$, are kept fixed both in shape and normalisation. Systematic studies at the Z peak when two jet $q\bar{q}$ events are forced into four jets show small discrepancies between data and Monte Carlo. This affects the $q\bar{q}$ background shape and is quantified using the 14 NN variables to yield a correction of $+50 \pm 50$ fb to the value from the fit. The corrected fit result is:

$$\sigma(WW \rightarrow q\bar{q}q\bar{q}) = 6.89 \pm 0.23(\text{stat.}) \pm 0.13(\text{syst.}) \text{ pb.}$$

If only events with a NN output greater than 0.3 are kept a value of 6.89 ± 0.23 pb is found showing no significant bias due to the $q\bar{q}$ background.

The sources contributing to the systematic uncertainty are summarised in Table 2. The largest contribution is the uncertainty in the $q\bar{q}$ background normalisation where a 5% variation is assumed. The contributions from uncertainties in the values of jet variables used in the event preselection and the NN input are assessed by adjusting their directions and energies according to residual differences observed between Z calibration data and Monte Carlo [19]. Possible miscalibrations of the calorimeters are also taken into account. The beam background is studied in the same way as described in section 2.2.1. The Monte Carlo statistics error is dominated by the 4f-CC03 correction.

Uncertainties in the WW generator are evaluated by comparing samples of fully simulated Monte Carlo events generated with KORALW and EXCALIBUR. To establish a WW fragmentation uncertainty, the HERWIG [20] generator was tuned at the Z peak both for all flavours and non-b quark flavors. Then, the same samples of signal events generated with KORALW are fragmented with both JETSET and the appropriately tuned HERWIG. For the $q\bar{q}$ background uncertainty, a sample of events generated with KORALZ using JETSET is compared with a separate sample of pure HERWIG events to assess the effect of the choice of generator. Colour reconnection effects are estimated using the SK1 model in JETSET with a reconnection probability of 0.3 and the effect of Bose-Einstein correlations is estimated according to the scheme, denoted BE₃, as proposed for the LUBOEI [21] implementation in JETSET. The procedures followed are the same as those used in Ref. [19].

Several cross checks have been performed on the fit result to search for possible biases arising in the selection and full simulation of the WW events. The previous version of the analysis with a different preselection and NN [1] gives 6.81 ± 0.23 pb. Another estimate with a preselection based mostly on charged tracks and a six variable NN using only charged tracks gives 6.83 ± 0.25 pb. Also, a selection based purely on calorimeter measurements with six input variables to a linear discriminant gives 6.91 ± 0.26 pb. A variety of linear discriminant analyses using from 4 to 14 variables give results which vary from 6.65 to 6.77 pb. All these checks give results which are consistently lower than the GENTLE prediction.

3 Total cross section

The total cross section is obtained from a fit to all channels described above assuming the Standard Model branching fractions, the only unknown being the total cross section. The fit uses the matrices of efficiencies and backgrounds for the various analyses and yields

$$\sigma_{\text{WW}} = 15.71 \pm 0.34(\text{stat.}) \pm 0.18(\text{syst.}) \text{ pb.}$$

Assuming no additional unexpected decay mode, the result is not significantly different if the branching fractions of the Standard Model decay modes are unconstrained.

The measurement is 5.5% lower than the GENTLE prediction. However, new calculations including full $\mathcal{O}(\alpha)$ electroweak corrections, calculable in the double pole approximation (DPA) [22] have recently appeared. Two Monte Carlo programs, YFSWW3 [23] and RacoonWW [24], are being developed. First numerical calculations find cross sections,

respectively, 1.9% [23] and 2.4% [24] lower than GENTLE at 189 GeV. The predictions from **RacoonWW** also include soft-photon exponentiation and leading log corrections for initial state radiation beyond $\mathcal{O}(\alpha)$ in addition to the calculations described in Ref. [24]. The uncertainty in the two new models is expected to be of the order of 0.5% [25].

Fig. 3 shows the total cross section measured as a function of the CM energy. The predictions of the two more complete YFSWW3 and **RacoonWW** calculations are also shown and are in better agreement with the experimental results than GENTLE. At 189 GeV, the measurement is 3.8% (1.5 standard deviations) below the YFSWW prediction and 3.2% (1.3 standard deviations) below the **RacoonWW** prediction. Taking into account also the cross section values measured by ALEPH [1] at 172 and 183 GeV, the data are $4.6 \pm 2.0\%$, $2.8 \pm 2.0\%$, and $2.3 \pm 2.0\%$ below the GENTLE, YFSWW and **RacoonWW** predictions respectively. These values use the signal efficiencies determined with KORALW and the quoted systematic uncertainty takes no account of any efficiency difference which may arise from the new calculations.

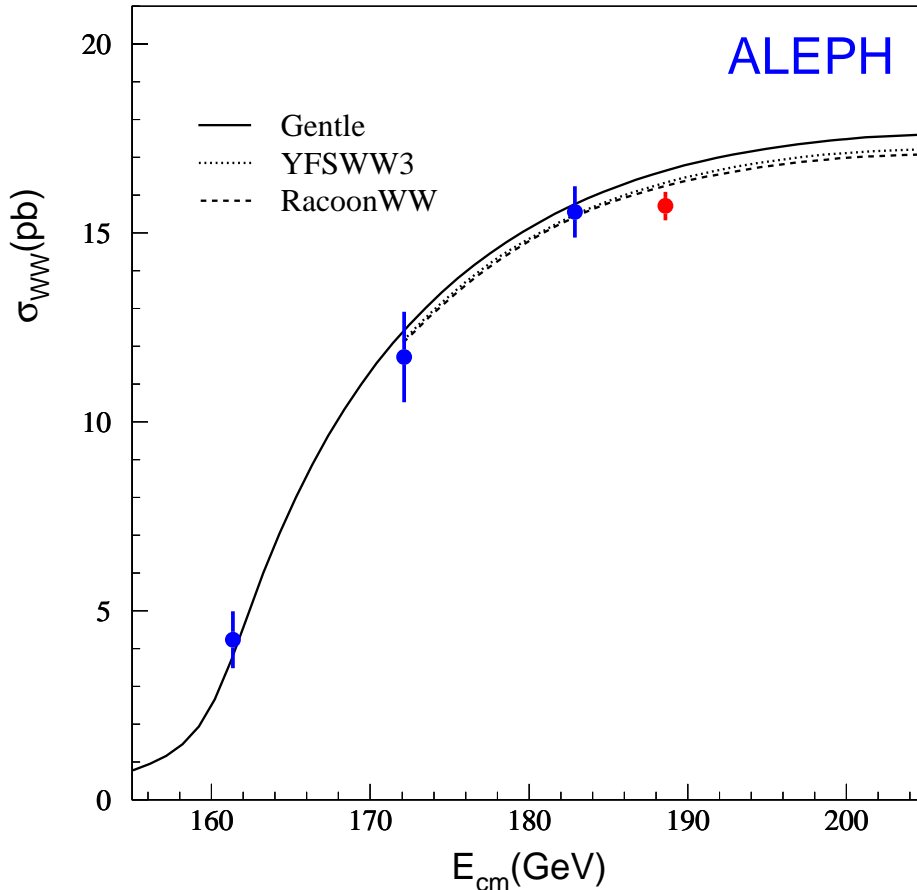


Figure 3: Measurements of the W-pair production cross section at four CM energies, compared with the Standard Model predictions from GENTLE, YFSWW3 and **RacoonWW**, for the LEP average value of the W mass [26].

4 Branching fractions and V_{cs}

The same fit as for the total cross section is performed combining the data samples collected at 161, 172, 183 and 189 GeV CM energies.

Without assuming lepton coupling universality, the seven unknowns are the three individual leptonic branching fractions and the four total cross sections at 161, 172, 183 and 189 GeV. The hadronic branching fraction is set to $1 - B_e - B_\mu - B_\tau$. The fitted leptonic branching fractions are

$$\begin{aligned} B(W \rightarrow e\nu) &= 11.35 \pm 0.46(\text{stat.}) \pm 0.17(\text{syst.})\%, \\ B(W \rightarrow \mu\nu) &= 11.10 \pm 0.44(\text{stat.}) \pm 0.16(\text{syst.})\%, \\ B(W \rightarrow \tau\nu) &= 10.51 \pm 0.55(\text{stat.}) \pm 0.22(\text{syst.})\%, \end{aligned}$$

and are consistent with lepton universality and the Standard Model expectations. Due to cross-contaminations in the identification of W decays to $\tau\nu$, $e\nu$ or $\mu\nu$, the measured $B(W \rightarrow \tau\nu)$ is 26% anticorrelated with $B(W \rightarrow e\nu)$ and 24% anticorrelated with $B(W \rightarrow \mu\nu)$. The $B(W \rightarrow e\nu)$ is 4.6% anticorrelated with $B(W \rightarrow \mu\nu)$.

If lepton universality is assumed a fit for $B(W \rightarrow q\bar{q})$ and the total cross sections at the four energies yields

$$B(W \rightarrow q\bar{q}) = 66.97 \pm 0.65(\text{stat.}) \pm 0.32(\text{syst.})\%.$$

This result can be expressed in terms of the individual couplings of the W to quark-antiquark pairs:

$$\frac{B(W \rightarrow q\bar{q})}{1 - B(W \rightarrow q\bar{q})} = (|V_{ud}|^2 + |V_{cd}|^2 + |V_{us}|^2 + |V_{cs}|^2 + |V_{ub}|^2 + |V_{cb}|^2)(1 + \alpha_s(m_W^2)/\pi). \quad (1)$$

The least well known of these is $|V_{cs}|$. Using the world average value of $\alpha_s(m_Z^2)$ evolved to m_W^2 , $\alpha_s(m_W^2) = 0.121 \pm 0.002$, and the squared sum of the other measured CKM matrix elements [27] which is 1.05 ± 0.01 , the measured hadronic branching fraction is

$$|V_{cs}| = 0.951 \pm 0.030(\text{stat.}) \pm 0.015(\text{syst.}).$$

5 Conclusions

The W-pair production cross section at $\sqrt{s} = 188.63$ GeV has been measured in all decay channels from an integrated luminosity of 174.20 pb^{-1} . The total cross section is found to be

$$\sigma_{WW} = 15.71 \pm 0.34(\text{stat.}) \pm 0.18(\text{syst.}) \text{ pb.}$$

This result is 5.5% (1.9 standard deviations) lower than the GENTLE prediction but in better agreement with more recent calculations. It agrees well with the recent measurement by the DELPHI Collaboration [28] at the same CM energy.

After inclusion of the data taken at CM energies of 161, 172 and 183 GeV, the hadronic decay branching fraction is found to be $66.97 \pm 0.65(\text{stat.}) \pm 0.32(\text{syst.})\%$ which is used to determine the CKM matrix element $|V_{cs}|$ equal to $0.951 \pm 0.030(\text{stat.}) \pm 0.015(\text{syst.}).$

Acknowledgements

We would like to thank S. Dittmaier and W. Placzek for helpful discussions on DPA. It is a pleasure to congratulate our colleagues from the CERN accelerator divisions for the successful operation of LEP at 189 GeV. We are indebted to the engineers and technicians in all our institutions for their contributions to the excellent performance of ALEPH. Those of us from non-member countries thank CERN for its hospitality.

Appendix: Neural network input variables for the $q\bar{q}q\bar{q}$ selection

The neural network hadronic event selection uses 14 variables. These are based on global event properties, heavy quark flavour tagging, jet properties and WW kinematics and are listed below. The four jets are numbered in order of decreasing energy.

Global event properties

- Thrust
- Sphericity
- Missing energy
- Sum of the four smallest interjet angles

Heavy flavour tagging

- Probability of an event being a light quark (uds) event based upon impact parameter significance of charged particles in the event

Jet properties

- Maximum electromagnetic energy fraction of a jet in any one degree cone
- Maximum summed charged particle energy fraction of a jet
- Minimum number of charged particles in a jet

WW kinematics

- Angle between Jet2 and Jet3

The following jet related variables are determined from kinematically fitted jet momenta.

- Energy of Jet1
- Energy of Jet3
- Energy of Jet4
- Smallest jet mass
- Second smallest jet mass

References

- [1] ALEPH Collaboration, *Measurement of the W mass in e^+e^- collisions at production threshold*, Phys. Lett. **B401** (1997) 347; *Measurement of W -pair cross section in e^+e^- collisions at 172 GeV*, Phys. Lett. **B415** (1997) 435; *Measurement of W -pair production in e^+e^- collisions at 183 GeV*, Phys. Lett. **B453** (1999) 107.
- [2] ALEPH Collaboration, *ALEPH: A detector for electron-positron annihilations at LEP*, Nucl. Inst. Meth. **A 294** (1990) 121.
- [3] ALEPH Collaboration, *Performance of the ALEPH detector at LEP*, Nucl. Inst. Meth. **A 360** (1995) 481.
- [4] ALEPH Collaboration, *Measurement of the absolute luminosity with the ALEPH detector*, Z. Phys. **C53** (1992) 375.
- [5] S. Jadach et al., Phys. Lett. **B253** (1991) 469; Phys. Lett. **B257** (1991) 173; Phys. Lett. **B260** (1991) 438; Comp. Phys. Commun. **70** (1992) 305. Also: S. Jadach, M. Melles, B.F.L. Ward and S.A. Yost, UTHEP-98-050.
- [6] The LEP Energy Working group, *Evaluation of the LEP Centre-of-Mass Energy for Data Taken in 1998*, LEP ECAL/99-01.
- [7] W. Beenakker and F.A. Berends, in *Physics at LEP2*, CERN 96-01, eds. G. Altarelli, T. Sjöstrand and F. Zwirner, Vol. 1, p. 79.
- [8] D. Bardin et al., Nucl. Phys. (Proc. Suppl.) **B37** (1994) 148; D. Bardin et al., Comp. Phys. Commun. **104** (1997) 161.
- [9] M. Skrzypek, S. Jadach, W. Placzek and Z. Wąs, Comp. Phys. Commun. **94** (1996) 216.
- [10] T. Sjöstrand, Comp. Phys. Commun. **82** (1994) 74.
- [11] F.A. Berends, R. Pittau and R. Kleiss, Comp. Phys. Commun. **85** (1995) 437.
- [12] J. Fujimoto et al., Comp. Phys. Commun. **100** (1997) 128.
- [13] S. Jadach, B.F.L. Ward and Z. Wąs, Comp. Phys. Commun. **79** (1994) 503.
- [14] T. Sjöstrand, Comp. Phys. Commun. **82** (1994) 74.
- [15] ALEPH Collaboration, *An experimental study of $\gamma\gamma \rightarrow$ hadrons at LEP*, Phys. Lett. **B313** (1993) 509.
- [16] S. Jadach et al., Phys. Lett. **B390** (1997) 298.
- [17] H. Anlauf et al., Comp. Phys. Commun. **79** (1994) 466.
- [18] Yu.L. Dokshitzer, J. Phys. **G17** (1991) 1441.

- [19] ALEPH Collaboration, *Measurement of the W mass and width in e^+e^- collisions at 189 GeV*, to be published in Eur. Phys. J. C
- [20] G. Marchesini et al., Comp. Phys. Commun. **67** (1992) 465.
- [21] L. Lönnblad and T. Sjöstrand, Eur. Phys. J. **C2** (1998) 165.
- [22] W. Beenakker, F.A. Berends and A.P. Chapovsky, Nucl. Phys. **B548** (1999) 3.
- [23] S. Jadach et al., Phys. Lett. **B417** (1998) 326; CERN-TH 99-222, UTHEP 98-0502, submitted to Phys. ReV. D.
- [24] A. Denner, S. Dittmaier, M. Roth and D. Wackerroth, “ $\mathcal{O}(\alpha)$ corrections to $e^+e^- \rightarrow WW \rightarrow 4$ fermions(+ γ): first numerical results from *RacoonWW*”, BI-TP 99/45, Dec. 1999, hep-ph/9912261.
- [25] S. Dittmaier, private communication and LEP2 Monte-Carlo Workshop, March 2000.
- [26] The LEP and SLD Collaborations, *A Combination of Preliminary Electroweak Measurements and Constraints on the Standard Model*, CERN-EP-2000-016, Jan. 2000.
- [27] C. Caso et al. (Particle Data Group), Review of Particles Physics, Eur. Phys. J. **C3** (1998) 1.
- [28] DELPHI Collaboration, *W pair production cross-section and branching fractions in e^+e^- interactions at 189 GeV*, CERN-EP-2000-035.